ELSEVIER

Journal of Chromatography A, 726 (1996) 193–204

JOURNAL OF CHROMATOGRAPHY A

Moving boundary electrophoretically mediated microanalysis

Bryan J. Harmon, Inkeun Leesong, Fred E. Regnier*

Purdue University, Department of Chemistry, West Lafayette, IN 47907-1393, USA

Received 3 April 1995; revised 29 August 1995; accepted 29 August 1995

Abstract

Moving boundary sample introduction is described as an alternative to zonal injection methods for the electrophoretically mediated microanalysis (EMMA) of leucine aminopeptidase (LAP). The capillary was initially filled with the analyte solution while the faster-migrating substrate, L-leucine-*p*-nitroanilide, was maintained in the inlet reservoir. Upon application of an electric field, electrophoretic merging of the reagents proceeded, and the detectable reaction product, *p*-nitroaniline, was transported to the detector. The area, maximum height, inclining slope, and declining slope of the resulting triangular product profile were each directly proportional to the activity of LAP, and the observed migration times of the product profile features defined the volume and time of the incubation. The moving boundary technique offered more than an order of magnitude greater concentration sensitivity than the zonal injection EMMA method. This heightened sensitivity facilitated rapid analysis as the use of elevated electric field strengths and short capillaries allowed for a 24-s kinetic determination of LAP.

Keywords: Sample introduction; Capillary electrophoresis; Electrophoretically mediated microanalysis; Leucine aminopeptidase; Enzymes

1. Introduction

Several recent reports [1–14] have described the use of capillary electrophoretic (CE) systems for reaction-based chemical analysis by a methodology known as electrophoretically mediated microanalysis (EMMA). In this technique, electrophoretic mixing is utilized to merge zones containing the analyte and its analytical reagent(s); the reaction is then allowed to proceed either in the presence or absence of an applied potential; and, finally, the reaction product is transported under the influence of an applied electric field to the detector. Thus, EMMA allows homogeneous kinetic enzyme assays [1–8] to be performed and detected entirely on-column with very high mass sensitivity due to the small dimensions of CE systems and the amplifying nature of enzymatic reactions. In potential applications such as rapid process monitoring or as a secondary dimension to a separation, it would be desirable to increase the speed with which EMMA analyses could be performed while retaining sensitivity.

Assuming that enzyme-saturating concentrations of substrate(s) are maintained, the concentration sensitivity of a kinetic enzyme assay can be approximated as:

$$\frac{\delta n_P}{\delta [E]} = k_{cat} V_{inc} t_{inc} \quad (1)$$

where n_P is the moles of product formed, [E] is the

*Corresponding author.

0021-9673/96/$15.00
SSDI 0021-9673(95)00969-8

concentration of enzyme active sites, k_{cat} is the turnover number of the enzyme for the chosen substrate, and V_{inc} and t_{inc} are the volume and time, respectively, of the incubation. As previously described [7], the incubation time for a zonal injection EMMA method performed at constant potential is typically limited to the time required for the analyte zone to migrate from the point of injection to the detection position

$$t_{inc} = \frac{l}{v_{net,A}} = \frac{l}{(\mu_{ep,A} + \mu_{eo})E} \quad (2)$$

where l is the separation length of the capillary; $v_{net,A}$ and $\mu_{ep,A}$ are the net migration velocity and electrophoretic mobility, respectively, of the analyte; μ_{eo} is the electroosmotic mobility; and E is the electric field strength. In traditional CE separations, analysis time can be decreased simply by either increasing the electric field strength or decreasing the separation length of the capillary with the restriction that Joule heating limits the separation efficiency [15]. As noted by Eqs. 1 and 2, increasing the speed of a kinetic EMMA enzyme determination in this manner also decreases its sensitivity since the time product is allowed to accumulate is concurrently decreased. However, Eq. 1 indicates that this loss in sensitivity can be counteracted by elevating the volume of analyte undergoing incubation.

Although CE has traditionally employed zonal injection methods, moving boundary CE has been reported by Pawliszyn and Wu [16,17] as an alternative sample introduction technique. There are two possible modes of moving boundary CE: leading edge and trailing edge. In the leading edge method, the capillary is initially filled with running buffer solution while analyte solution is maintained in the inlet buffer reservoir. Upon application of an electric field, sample components continuously enter the capillary at their characteristic net migration velocities, and the resulting electropherogram consists of upward stairsteps as the leading edge of each succeeding region containing a detectable species is superimposed upon those which have already reached the detector. In the trailing edge technique, the capillary is initially filled with analyte solution while running buffer solution is maintained in the inlet reservoir. Upon application of an electric field, sample components exit the capillary with their characteristic net migration velocities, and the resulting electropherogram consists of downward stairsteps representing the migration of the trailing edges of each detectable analyte zone past the detection position. This study investigates moving boundary sample introduction as a method to increase the incubation volume and, consequently, the sensitivity of kinetic EMMA enzyme assays.

The model analysis chosen for this study was the kinetic determination of microsomal leucine aminopeptidase (LAP; EC 3.4.1.1). LAP was assayed by its hydrolysis of L-leucine-*p*-nitroanilide to form *p*-nitroaniline and L-leucine. Therefore, LAP and L-leucine-*p*-nitroanilide served as the analyte and analytical reagent, respectively, while *p*-nitroaniline was monitored at its unique absorbance of 405 nm as the detectable product.

2. Experimental

2.1. Instrumentation

All experiments were performed using a BioFocus 3000 capillary electrophoresis system (Bio-Rad Laboratories, Hercules, CA, USA). Polyimide-coated fused-silica capillaries (Polymicro Technologies, Phoenix, AZ, USA) of 50 μm I.D.×360 μm O.D. and total lengths of 24 cm were utilized. The separation lengths were 19.4 and 4.6 cm for the determinations of LAP depicted in Fig. 1 and Fig. 4, respectively.

2.2. Reagents

Porcine kidney microsomal LAP and L-leucine-*p*-nitroanilide were purchased from Sigma (St. Louis, MO, USA). Monobasic and dibasic potassium phosphate and methanol were obtained from Fisher Scientific (Fair Lawn, NJ, USA). The analytical reagent solution was made by dissolving 4 m*M* L-leucine-*p*-nitroanilide and 5% (v/v) methanol in 25 m*M* phosphate buffer solution and adjusting to pH 7.2 with 1.0 *M* HCl or 1.0 *M* NaOH. The analyte solutions were prepared by dissolving LAP in pH 7.2 25 m*M* phosphate buffer solution.

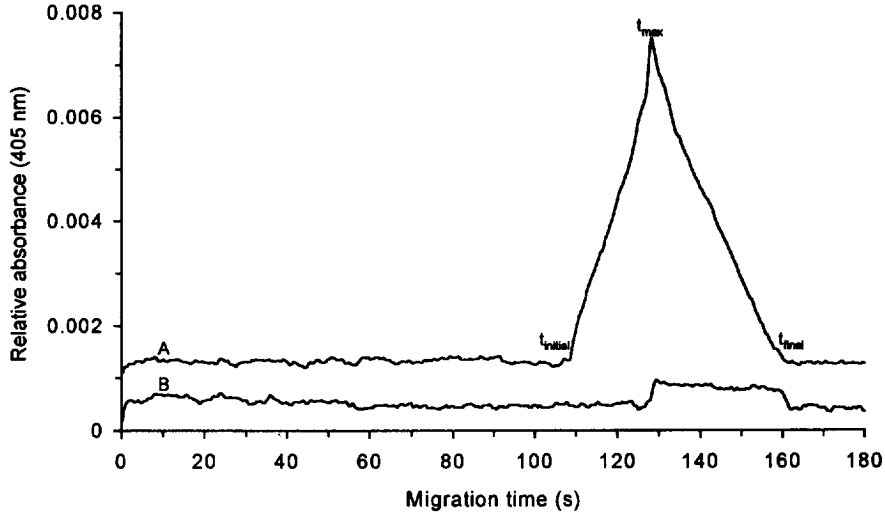

Fig. 1. (A) Moving boundary and (B) 5 nl zonal injection kinetic EMMA determinations of 28.5 μg ml^{-1} solution of LAP. For conditions see text.

2.3. Procedures

For moving boundary EMMA determinations of LAP, the capillary was initially filled with analyte solution while analytical reagent solution was maintained in the anodic buffer reservoir. For zonal injection EMMA determinations of LAP, the capillary was initially filled with pH 7.2 25 m*M* phosphate buffer solution, analyte solution was injected at the anodic inlet by the application of pressure, and analytical reagent solution was maintained in the anodic buffer reservoir. Assays were effected by applying an electric field (300 V cm^{-1} for Fig. 1 and 500 V cm^{-1} for Fig. 4) and monitoring the absorbance at 405 nm. The capillary was thermostatted by circulating water at 25°C throughout each assay. Between determinations, the capillary was purged with 0.1 *M* KOH and refilled by pressure with the appropriate solution.

3. Results and discussion

Conventional reaction-based chemical analysis requires four steps: (1) analyte and analytical reagent metering; (2) initiation of reaction; (3) control of reaction conditions and product formation; and (4) detection of product. The following discussion describes the theoretical basis which allowed moving boundary EMMA to perform these necessary tasks for the kinetic determination of LAP with specific references to the assay depicted in Fig. 1.

3.1. Analyte and analytical reagent metering

In moving boundary EMMA, the initial positioning of the analyte and analytical reagent zones is determined by the relative electrophoretic mobilities of the reagent species so that their respective regions interpenetrate under the influence of an applied electric field. Consequently, the capillary is initially filled with the reagent (i.e. enzyme or substrate) of lower net migration velocity (termed the 'fill' reagent) while the inlet buffer reservoir contains the reagent (i.e. complementary substrate or enzyme of the fill reagent) of greater net migration velocity (termed the 'frontal' reagent). As indicated by the experimental electrophoretic properties listed in Table 1, L-leucine-*p*-nitroanilide demonstrated a greater net mobility than LAP. Consequently, analytical reagent solution was maintained in the anodic inlet buffer reservoir while the capillary was initially filled with analyte solution.

Table 1
Electrophoretic properties of chemical species involved in moving boundary EMMA determination of LAP

Chemical species	Electrophoretic mobility ($cm^2 V^{-1} s^{-1}$)	Net mobility[a] ($cm^2 V^{-1} s^{-1}$)
Leucine aminopeptidase	$-1.0 \cdot 10^{-4}$	$4.0 \cdot 10^{-4}$
Leucine-*p*-nitroanilide	$1.0 \cdot 10^{-4}$	$6.0 \cdot 10^{-4}$
p-Nitroaniline	~0	$5.0 \cdot 10^{-4}$

[a] Sum of electrophoretic and electroosmotic mobilities.

3.2. Initiation of reaction

Following metering of the fill and frontal reagents in appropriate positions, electrophoretic mixing of the analyte and analytical reagents and, thus, the analytical reaction are initiated in moving boundary EMMA by the application of an electric field. The boundary of the faster-migrating frontal reagent zone entering the capillary from the inlet reservoir electrophoretically interpenetrates the slower-migrating fill reagent zone initially contained in the capillary. Since LAP and L-leucine-*p*-nitroanilide were metered adjacently for the determination depicted in Fig. 1, their electrophoretic mixing commenced immediately upon the application of potential. However, as observed in zonal injection EMMA methods [1,7], diffusional interpenetration and concurrent reaction occurred at the interface between the adjacent reagent zones prior to the application of the electric field. This phenomenon could be prevented by injecting a plug of buffer between the frontal and fill reagent zones sufficiently broad to prevent their diffusional mixing.

3.3. Control of reaction conditions and product formation

Upon electrophoretic mixing, the merged region extends from the trailing edge of the fill reagent zone to the leading edge of the frontal reagent zone. As an electric field is maintained for time t, the width of this reagent overlap ($d_{overlap}$) can be estimated as:

$$d_{overlap} = (v_{net,frontal} - v_{net,fill})\, t = (\mu_{ep,frontal} - \mu_{ep,fill})\, E\, t \quad (3)$$

where $v_{net,frontal}$ and $\mu_{ep,frontal}$ are the net migration velocity and electrophoretic mobility, respectively, of the frontal reagent, and $v_{net,fill}$ and $\mu_{ep,fill}$ are the net migration velocity and electrophoretic mobility, respectively, of the fill reagent. Fig. 2 depicts this reagent overlap as a function of distance from the anodic inlet and time of the constant applied electric field for the determination depicted in Fig. 1. The net migration velocities of the leading edge of the frontal reagent zone (i.e. 0.18 cm s^{-1}) and the trailing edge of the fill reagent zone (i.e. 0.12 cm s^{-1}) are represented by vectors A and B, respectively, in Fig. 2. Therefore, the regions of the capillary below the $v_{net,frontal}$ vector and above the $v_{net,fill}$ vector contain the frontal reagent and the fill reagent, respectively, and the area contained between these two boundaries represents the spatial positioning of the overlap of the two reagent zones as a function of the time potential was applied. Since *p*-nitroaniline was transported from the injection inlet toward the detector under the influence of an electric field, only product which was formed within the merged region prior to or at the detection position could be monitored. Any product which was formed at a position beyond the detector was not observable under the influence of a constant potential. Consequently, the moving boundary EMMA method provided an incubation of fixed time and volume determined by the overlap of the fill and frontal reagent zones prior to passing by the detection position. This observable reagent overlap is depicted as the shaded triangular area in Fig. 2 which is bounded by the vectors representing the migration of the leading and trailing edges of the frontal and fill reagent zones, respectively, and the horizontal line corresponding to the detection position (i.e. 19.4 cm; indicated by C). The area of this triangular region and, consequently, the distance·time product

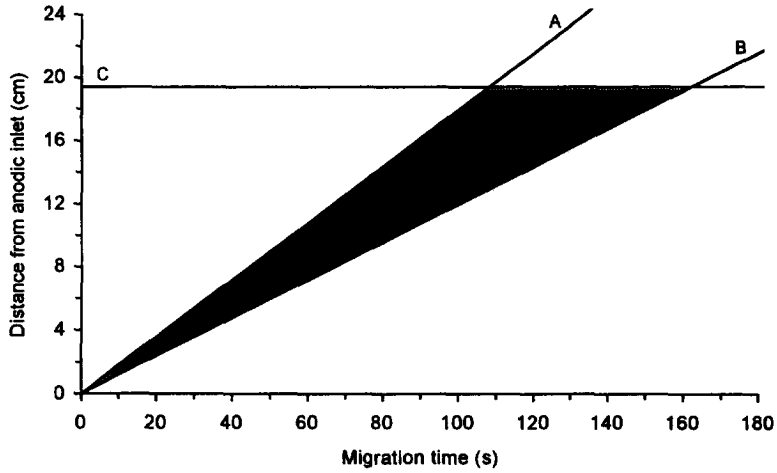

Fig. 2. Reagent overlap for moving boundary EMMA determination of LAP depicted in Fig. 1. (A), migration of leading edge of frontal reagent zone; (B), migration of trailing edge of fill reagent zone; (C), detection position. Shaded area represents observable reagent overlap region.

of the detectable incubation ($d_{inc}t_{inc}$) is:

$$d_{inc}\,t_{inc} = \frac{l}{2}\left(\frac{l}{v_{net,fill}} - \frac{l}{v_{net,frontal}}\right) = \frac{(\mu_{ep,frontal} - \mu_{ep,fill})\,l^2}{2\,(\mu_{ep,frontal} + \mu_{eo})\,(\mu_{ep,fill} + \mu_{eo})\,E} \quad (4)$$

The total moles of product formed within the observable reagent overlap are equal to the product of the distance·time product of the detectable incubation, the cross-sectional area of the capillary, and the velocity of the reaction within the merged region (v_{rxn}):

$$n_P = d_{inc}\,t_{inc}\,\pi\,r^2\,v_{rxn} \quad (5)$$

where r is the radius of the capillary. Assuming that an enzyme-saturating concentration of substrate is maintained within the observable reagent overlap, the rate of reaction remains relatively constant and directly proportional to the activity of the enzyme:

$$v_{rxn} = k_{cat}\,[E] \quad (6)$$

and, therefore:

$$n_P = \frac{(\mu_{ep,frontal} - \mu_{ep,fill})\,l^2\,\pi\,r^2}{2\,(\mu_{ep,frontal} + \mu_{eo})\,(\mu_{ep,fill} + \mu_{eo})\,E}\,k_{cat}\,[E] \quad (7)$$

Eq. 7 indicates that the amount of product observed in the moving boundary EMMA determination of an enzyme serves as a kinetic measure of the activity of the enzyme solution. However, in contrast to zonal injection EMMA techniques, the moving boundary method does not require knowledge of an injection volume since it is the electrophoretic properties of the system as well as the electric field strength and separation length of the capillary which determine both the volume and time of the incubation. Furthermore, as described in the following section, the volume and time of the incubation can be readily calculated from the observed product profile.

3.4. Detection of product

In moving boundary EMMA, non-reacting species display the upward or downward stairstep profiles typical of leading edge or trailing edge moving boundary CE depending upon whether they are initially contained in the frontal or fill reagent zone, respectively. However, as depicted in Fig. 1, the concentration profile of the reaction product is triangular. This unique profile results from the triangular observable reagent overlap previously described. Although all observed product possesses a similar electrophoretic mobility, the time at which specific product is detected is dependent upon the

time and position it was formed within the reagent overlap region. As a result, the migration times observed for the product profile are determined by the net migration velocities of the frontal and fill reagents as well as of the product. As shown in Fig. 3, since L-leucine-*p*-nitroanilide had a greater net migration velocity than either *p*-nitroaniline or LAP, the first product to reach the detector was that which formed just as the leading edge of the frontal reagent zone migrated past the detection position. Consequently, the initial observed product essentially traversed the entire separation length of the capillary with the net migration velocity of the frontal reagent and was observed at a corresponding time ($t_{initial}$) of:

$$t_{initial} = \frac{l}{v_{net,frontal}} = \frac{l}{(\mu_{ep,frontal} + \mu_{eo})E} \quad (8)$$

Since LAP possessed the lowest net migration velocity of the three species, the last product that could be observed was that which formed as the trailing edge of the fill reagent zone migrated past the detector. Therefore, the final detected product essentially traversed the entire separation distance of the capillary with the net migration velocity of the fill reagent and was observed at a corresponding time (t_{final}) of:

$$t_{final} = \frac{l}{v_{net,fill}} = \frac{l}{(\mu_{ep,fill} + \mu_{eo})E} \quad (9)$$

Any *p*-nitroaniline formed after the trailing edge of the fill reagent zone passed by the detection position could not be monitored under the influence of a fixed electric field. Assuming that the rate of reaction was constant within the observable reagent overlap region, the greatest accumulation of product which arrived simultaneously at the detection position was formed at times and positions coincident with a vector representing the net migration velocity of the product (i.e. 0.15 cm s^{-1}; D in Fig. 3). Therefore, the maximum accumulation in the product profile was observed at a time (t_{max}) indicative of the net migration velocity of the product:

$$t_{max} = \frac{l}{v_{net,P}} = \frac{l}{(\mu_{ep,P} + \mu_{eo})E} \quad (10)$$

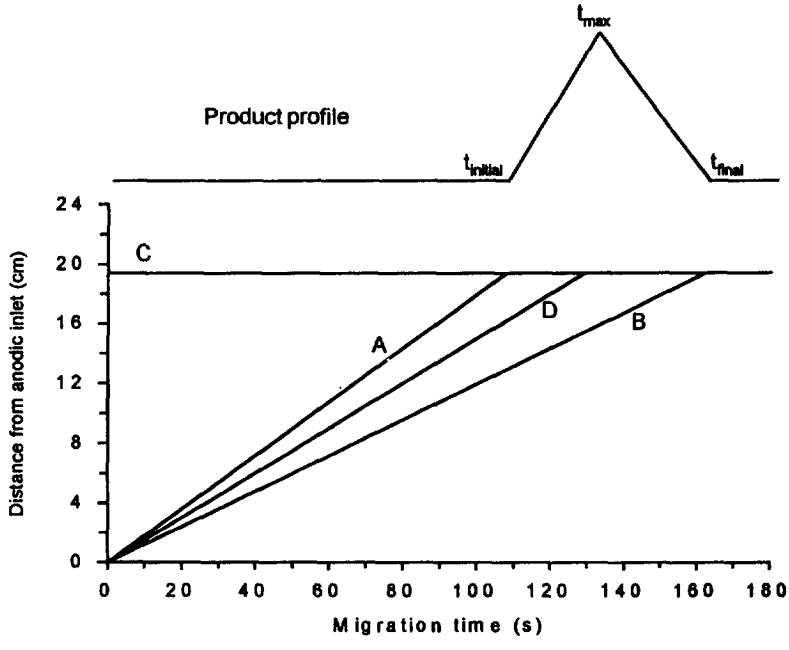

Fig. 3. Observed migration times of product profile features for moving boundary EMMA determination of LAP depicted in Fig. 1. (A), migration of leading edge of frontal reagent zone; (B), migration of trailing edge of fill reagent zone; (C), detection position; (D), migration of maximal accumulation of product.

where $v_{net,P}$ and $\mu_{ep,P}$ are the net migration velocity and electrophoretic mobility, respectively, of the product. As a result, the features of the observed product profile (i.e. $t_{initial}$, t_{max}, and t_{final}) in Fig. 1 correspond to the net migration velocities of L-leucine-*p*-nitroanilide, *p*-nitroaniline, and LAP, respectively.

In a similar manner, for systems in which the net migration velocity of the product is greater than those of the frontal and fill reagent zones, $t_{initial}$, t_{max}, and t_{final} in the triangular product profile correspond to the net migration velocities of the product, frontal reagent, and fill reagent, respectively. In systems for which the product has the slowest net migration velocity, $t_{initial}$, t_{max}, and t_{final} are determined by the net migration velocities of the frontal reagent, fill reagent, and product, respectively. Consequently, net mobilities (i.e. $\mu_{ep,n}+\mu_{eo}$) of the frontal and fill reagents and product can be estimated for each moving boundary EMMA determination from the detection times of the corresponding features in the observed product profile:

$$\mu_{ep,n} + \mu_{eo} = \frac{l}{E\, t_n} \tag{11}$$

where t_n is the detection time of the product profile feature corresponding to species n. As a result, the distance·time product of the observable reagent incubation can be estimated from the product profile by substitution of Eq. 11 into Eq. 4:

$$d_{inc}\, t_{inc} = \frac{(t_{fill} - t_{frontal})\, l}{2} \tag{12}$$

where t_{fill} and $t_{frontal}$ are the detection times of the product profile features corresponding to the net migration velocities of the fill and frontal reagent zones, respectively. Eq. 12 estimated that the moving boundary determination depicted in Fig. 1 offered an observable incubation of approximately 524 cm s (i.e. 10.3 μl s).

The volume occupied by the resulting product can be calculated as the product of the volumetric velocity of the product and the temporal width of its profile (i.e. $t_{final}-t_{initial}$):

$$V_P = \pi r^2 v_{net,P} (t_{final} - t_{initial})$$
$$= \frac{\pi r^2 l (\mu_{ep,fast} - \mu_{ep,slow})(\mu_{ep,P} + \mu_{eo})}{(\mu_{ep,fast} + \mu_{eo})(\mu_{ep,slow} + \mu_{eo})} \tag{13}$$

where $\mu_{ep,fast}$ and $\mu_{ep,slow}$ are the electrophoretic mobilities of the species of greatest and least net migration velocity (i.e. responsible for $t_{initial}$ and t_{final}), respectively, or, in terms of the features of the product profile:

$$V_P = \frac{\pi r^2 l (t_{final} - t_{initial})}{t_P} \tag{14}$$

where t_P is the detection time of the product profile feature corresponding to the net migration velocity of the product. Eq. 14 estimated that the volume of the product profile for the moving boundary determination depicted in Fig. 1 was approximately 0.16 μl.

The average molarity of the product profile ($M_{P,avg}$) is equal to the ratio of the total observable moles of product to the volume of its profile:

$$M_{P,avg} = \frac{n_P}{V_P}$$
$$= \frac{(\mu_{ep,frontal} - \mu_{ep,fill})\, l}{2(\mu_{ep,fast} - \mu_{ep,slow})(\mu_{ep,intermediate} + \mu_{eo})\, E}$$
$$\times k_{cat}\,[E] \tag{15}$$

where $\mu_{ep,intermediate}$ is the electrophoretic mobility of the species of intermediate net migration velocity (i.e. responsible for t_{max}) or, in terms of the features of the product profile:

$$M_{P,avg} = \frac{t_P (t_{fill} - t_{frontal})}{2 (t_{final} - t_{initial})} k_{cat}\,[E] \tag{16}$$

If detection is achieved by monitoring the absorbance of the product, the average height of the product profile ($h_{P,avg}$; in units of relative absorbance) can be approximated by application of the Beer–Lambert Law to Eq. 16:

$$h_{P,avg} = \epsilon_P\, b\, M_{P,avg} = \epsilon_P\, b$$
$$\times \frac{(\mu_{ep,frontal} - \mu_{ep,fill})\, l}{2(\mu_{ep,fast} - \mu_{ep,slow})(\mu_{ep,intermediate} + \mu_{eo})\, E}$$
$$\times k_{cat}\,[E] \tag{17}$$

where ϵ_P is the molar absorptivity of the product, and b is the cell path length, or, in terms of the features of the product profile:

$$h_{P,avg} = \epsilon_P\, b \frac{t_P (t_{fill} - t_{frontal})}{2 (t_{final} - t_{initial})} k_{cat}\,[E] \tag{18}$$

The maximum height of the triangular product profile ($h_{P,max}$) is simply equal to twice its average height:

$$h_{P,max} = 2\,h_{P,avg} = \epsilon_P\, b \times \frac{(\mu_{ep,frontal} - \mu_{ep,fill})\, l}{(\mu_{ep,fast} - \mu_{ep,slow})\,(\mu_{ep,intermediate} + \mu_{eo})\, E} \times k_{cat}\,[E] \quad (19)$$

or, in terms of the features of the product profile:

$$h_{P,max} = \epsilon_P\, b\, \frac{t_P\,(t_{fill} - t_{frontal})}{t_{final} - t_{initial}}\, k_{cat}\,[E] \quad (20)$$

Consequently, the maximum height of the product profile is directly proportional to the activity of the enzyme, and the sensitivity of this quantitation method is directly proportional to the turnover number of the enzyme and separation length of the capillary and inversely proportional to the electric field strength.

The total area of the product profile (A_P) is equal to the product of its average height and temporal width:

$$A_P = h_{P,avg}\,(t_{final} - t_{initial}) = \epsilon_P\, b \times \frac{(\mu_{ep,frontal} - \mu_{ep,fill})\, l^2}{2\,(\mu_{ep,fast} + \mu_{eo})\,(\mu_{ep,intermediate} + \mu_{eo})\,(\mu_{ep,slow} + \mu_{eo})\, E^2} \times k_{cat}\,[E] \quad (21)$$

or, in terms of the features of the product profile:

$$A_P = \epsilon_P\, b\, \frac{t_P\,(t_{fill} - t_{frontal})}{2}\, k_{cat}\,[E] \quad (22)$$

Therefore, the area of the product profile is directly proportional to the activity of the enzyme, and the sensitivity of this quantitation method is directly proportional to the turnover number of the enzyme and square of the separation length of the capillary and indirectly proportional to the square of the electric field strength.

The slope of the inclining region ($m_{incline}$) of the triangular product profile is obtained by dividing the maximum product profile height by the difference in detection times between the species of intermediate and greatest net migration velocity:

$$m_{incline} = \frac{h_{P,max}}{t_{max} - t_{initial}} = \epsilon_P\, b \times \frac{(\mu_{ep,fast} + \mu_{eo})\,(\mu_{ep,frontal} - \mu_{ep,fill})}{(\mu_{ep,fast} - \mu_{ep,slow})\,(\mu_{ep,fast} - \mu_{ep,intermediate})} \times k_{cat}\,[E] \quad (23)$$

or, in terms of the features of the product profile:

$$m_{incline} = \epsilon_P\, b\, \frac{t_P\,(t_{fill} - t_{frontal})}{(t_{final} - t_{initial})\,(t_{max} - t_{initial})}\, k_{cat}\,[E] \quad (24)$$

In a similar manner, the declining slope ($m_{decline}$) of the triangular product profile is obtained by dividing the maximum peak height by the difference in detection times between the species of intermediate and least net migration velocity:

$$m_{decline} = \frac{h_{P,max}}{t_{max} - t_{final}} = \epsilon_P\, b \times \frac{(\mu_{ep,slow} + \mu_{eo})\,(\mu_{ep,frontal} - \mu_{ep,fill})}{(\mu_{ep,fast} - \mu_{ep,slow})\,(\mu_{ep,slow} - \mu_{ep,intermediate})} \times k_{cat}\,[E] \quad (25)$$

or, in terms of the features of the product profile:

$$m_{decline} = \epsilon_P\, b\, \frac{t_P\,(t_{fill} - t_{frontal})}{(t_{final} - t_{initial})\,(t_{max} - t_{final})}\, k_{cat}\,[E] \quad (26)$$

Consequently, the inclining and declining slopes of the product profile are directly proportional to the activity of the enzyme. The sensitivity of this quantitation method is directly proportional to the turnover number of the enzyme and independent of the separation length of the capillary and electric field strength.

As previously indicated, the product profile maximum height, area, inclining slope, and declining slope are each directly proportional to the enzymatic activity, and, since the observed migration times of the product profile features define the volume and time of the incubation, activity can be directly calculated on a volumetric basis without knowledge of an injection volume. The product profile depicted in Fig. 1 offered values of approximately 0.0060 AU, 0.146 AU s, $2.53 \cdot 10^{-4}$ AU s^{-1}, and $-1.67 \cdot 10^{-4}$ AU

s^{-1}, respectively, for these quantitation parameters, which yielded similar LAP activities of 0.18, 0.16, 0.16, and 0.16 U ml^{-1}, respectively, as calculated by Eqs. 20, 22, 24, and 26, respectively. The elevated LAP activity determined by use of the product profile maximum height could be attributed to the comigration at t_{max} of the maximal accumulation of product with the additional product formed at the reagent interface prior to the application of the electric field. Due to its ease of calculation, product profile area is typically the quantitation method of choice. However, the other quantitation techniques may be preferable in specific applications, such as when matrix interferants comigrate with a portion of the product profile. Inclining slope can also be exploited for fast analyses since the determination of the complete product profile is not required.

3.5. Assumptions of mathematical model

The simple mathematical model presented for moving boundary EMMA primarily accounts for the effects of electromigration of the enzyme, substrate, and product zones upon the observed concentration profile of the product. Other potentially important phenomena are neglected by the model, including diffusion, whose contribution is most obvious in the product accumulation formed at the reagent interface prior to the application of potential. Furthermore, it is assumed that the enzyme zone traverses the entire capillary with a fixed net migration velocity. However, when enzyme and substrate regions merge, a certain proportion of the enzyme is sequestered in an enzyme–substrate complex. It has been previously observed that the electrophoretic mobility of an enzyme–substrate complex can differ significantly from that of the uncomplexed form [1,5,18,19]. However, the enzyme–substrate complex of LAP did not exhibit this phenomenon (i.e. in the presence of varying concentrations of L-leucine-*p*-nitroanilide, the migration time of the enzyme did not demonstrate a significant substrate concentration dependence). As a result, no corrections were made for variable electrophoretic mobility of the merged reagent zone.

It is further assumed that the conductivities of the frontal and fill reagent zones and merged reagent region are similar, and, therefore, the potential gradient is constant throughout the capillary. However, moving boundary techniques may be viewed as continuous electrokinetic injections. In electrokinetic sample introduction methods, if the sample and running buffer zones exhibit dissimilar conductivities, electric field strengths within their respective regions are also unequal. This phenomenon has been exploited in sample 'stacking' techniques to concentrate analytes at interfaces of zones of dissimilar conductivity [20–22]. If the frontal and fill reagent zones as well as the merged reagent region are of significantly differing conductivities, solute stacking effects are expected to also occur in moving boundary EMMA thereby resulting in skewing of the triangular product profile. However, in the determinations of LAP, the frontal and fill reagent zones were of similar conductivities, and significant effects of variable potential gradients within the reagent zones and merged reagent region were not observed.

3.6. Reproducibility and linearity of moving boundary EMMA method

Fifteen replicate determinations of a LAP sample containing 28.5 $\mu g\ ml^{-1}$ were made to evaluate the reproducibility of the moving boundary EMMA assay utilizing the experimental conditions of Fig. 1. Quantitation based upon areas of the *p*-nitroaniline profiles yielded a R.S.D. of 5.4%. However, when quantitation was based upon LAP activities calculated from the observed product profile areas and the migration times of the product profile features (i.e. Eq. 22), the R.S.D. improved to 3.9%. This quantitation technique demonstrated increased precision due to its inherent compensation for run-to-run variability in both the time and volume of the observable incubation and the velocity with which the product migrates past the detection position. In this manner, moving boundary EMMA does not require an internal standard as is typically utilized in zonal injection methods to compensate for variability in injection volume. The migration times of the features of the product profile (i.e. $t_{initial}$, t_{max}, and t_{final}) exhibited R.S.D.s of 0.54%, 0.55%, and 0.91%, respectively.

Calibration curves were constructed for the moving boundary EMMA determination of five LAP samples ranging from 3.6 to 57 $\mu g\ ml^{-1}$ utilizing the experimental conditions for Fig. 1. Five replicate

assays were performed for each sample. When quantitation was based upon areas of the product profiles, the linear range extended throughout the sample range, and linear regression of the data yielded $A_P = 5.35 \cdot 10^{-3}\ C_{LAP} - 4.2 \cdot 10^{-4}$ AU s^{-1} with a correlation coefficient of 0.9991. When quantitation was based upon LAP activities calculated from the product profile areas and the observed migration times of the product profile features (i.e. Eq. 22), the linear range also extended throughout the sample range, and linear regression of the data produced $k_{cat}[E] = 5.83 \cdot 10^{-3}\ C_{LAP} - 2.18 \cdot 10^{-3}$ U ml^{-1} with a correlation coefficient of 0.9998. The method offered a lower limit of detection of approximately 0.2 μg ml^{-1} (i.e. 1 mU ml^{-1}).

3.7. Comparison to zonal injection EMMA method

Fig. 1 and Table 2 offer a comparison of constant potential EMMA determinations of LAP utilizing moving boundary and zonal injection sample introduction while keeping all other experimental parameters identical. As previously described [7], the zonal injection method resulted in a plateau of product extending between detection times corresponding to the net migration velocities of the product and analyte. Eq. 2 estimated that the 5-nl zonal injection method offered an incubation time of 162 s and, therefore, an observable incubation of approximately 0.8 μl s, more than an order of magnitude less than that obtained by the moving boundary technique. As shown in Table 2, the enhanced reagent overlap of the moving boundary assay was reflected in the concentration sensitivities of the two methods. Based upon the slopes of calibration curves, the moving boundary technique yielded more than an order of magnitude greater concentration sensitivity for both product profile height and area. Since the final observed product was determined by the net migration velocity of LAP for both sample introduction methods, their analysis times were similar. However, since the volume of analyte required for the moving boundary technique was equal to the volume of the capillary, the consumption of analyte per assay was nearly two orders of magnitude greater than for the zonal injection method.

3.8. Fast moving boundary EMMA

As previously noted, decreased analysis time can be achieved at the expense of sensitivity by utilizing elevated electric field strengths and short separation distances. Table 3 details the effect of electric field strength upon moving boundary EMMA determinations of a 28.5-μg ml^{-1} sample of LAP at electric field strengths of 100 to 400 V cm^{-1} and confirms the electric field dependences predicted by the mathematical models for various experimental parameters. Although the migration time of the final observed product and, thus, the analysis time were inversely proportional to the electric field strength, the observable incubation displayed the same electric field dependence. As a result, concurrent losses in sensitivity were observed when analysis time was minimized.

Although decreased analysis time results in diminished sensitivity as in all kinetic EMMA methods, the inherent greater concentration sensitivity of the moving boundary technique permits analyses to be performed faster than by zonal injection methods

Table 2
Comparison of moving boundary and zonal injection EMMA determinations of LAP

Parameter	Moving boundary EMMA	Zonal injection EMMA
Consumption of analyte (nl)	470	5
Analysis time (s)	162	162
Observable reagent overlap (μl s)	10.3	0.8
Sensitivity of quantitation method		
Product signal height (AU ml μg^{-1})	$2.0 \cdot 10^{-4}$	$1.3 \cdot 10^{-5}$
Product signal area (AU s ml μg^{-1})	$5.4 \cdot 10^{-3}$	$4.4 \cdot 10^{-4}$

Table 3
Effects of electric field strength upon moving boundary EMMA kinetic determinations of LAP

E (V cm^{-1})	$t_{initial}$ (s)	t_{max} (s)	t_{final} (s)	$d_{inc}t_{inc}$ (cm s)	A_P (AU s)	h_P (AU)	$m_{incline}$ (AU s^{-1})	$m_{decline}$ (AU s^{-1})
100	340	405	501	1560	1.38	0.0172	$2.5{\cdot}0^{-4}$	$-1.7{\cdot}10^{-4}$
150	222	262	328	1030	0.574	0.0108	$2.7{\cdot}0^{-4}$	$-1.6{\cdot}10^{-4}$
200	166	199	248	795	0.356	0.0084	$2.5{\cdot}0^{-4}$	$-1.7{\cdot}10^{-4}$
300	108	130	160	504	0.164	0.0061	$2.4{\cdot}0^{-4}$	$-1.8{\cdot}10^{-4}$
400	78	95	119	398	0.093	0.0043	$2.5{\cdot}0^{-4}$	$-1.8{\cdot}10^{-4}$
Theoretical E^n [a]	−1	−1	−1	−1	−2	−1	0	0
R^2 [b]	0.9999	0.9996	0.9998	0.9992	0.998	0.995	–	–
Experimental E^n [c]	−1.06	−1.04	−1.04	−1.00	−1.92	−0.96	−0.01	0.06

[a] Theoretical electric field dependence of experimental parameter expressed as coefficient of electric field strength in theoretical equations.
[b] Correlation coefficient obtained for linear regression of experimental parameter vs. theoretical electric field dependence.
[c] Experimental electric field dependence of experimental parameter determined by slope of plot of logarithm of appropriate experimental value vs. logarithm of electric field strength.

with similar concentration sensitivity. As depicted in Fig. 4, the use of a 4.6-cm separation distance and an electric field strength of 500 V cm^{-1} allowed for the kinetic determination of LAP in 24 s. A 1-nl zonal injection method required an analysis time of approximately 420 s to obtain a similar product profile height and area sensitivity. Fifteen replicate assays yielded a R.S.D. of 2.7% for quantitation based upon product profile area, and a lower limit of detection of approximately 2 μg ml^{-1} (i.e. 10 mU ml^{-1}) was observed for the conditions shown in Fig. 4.

4. Conclusions

Moving boundary sample introduction has demonstrated enhanced concentration sensitivity relative to zonal sample introduction thereby allowing kinetic enzyme assays to be performed an order of magnitude faster. However, due to its greater sample requirement, the moving boundary method typically offers lesser mass sensitivity. Furthermore, the volume and time of the observable incubation for moving boundary EMMA are defined by the ob-

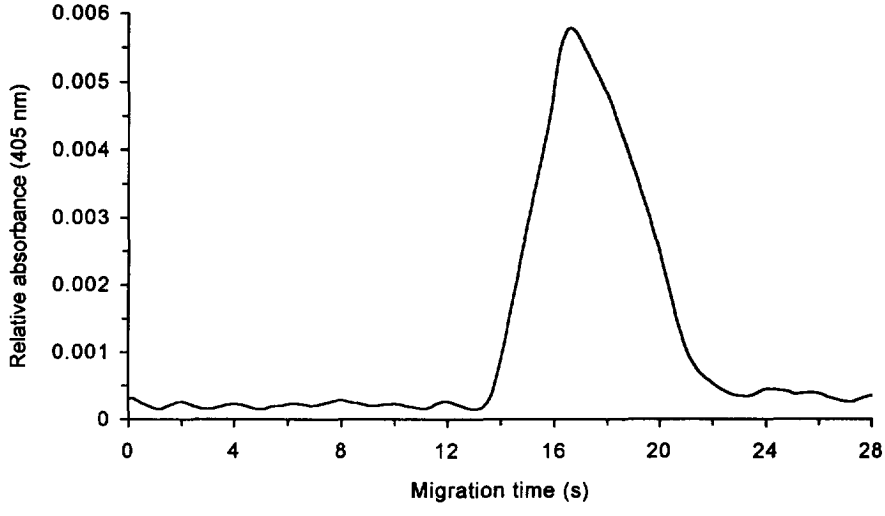

Fig. 4. Fast-moving boundary EMMA determination of LAP. For conditions see text.

served migration times of the triangular product profile thereby eliminating the need for an internal standard to compensate for variability in injection volume. However, the invariant migration times of the product profile do not allow for the selective control of product detection times previously described for zonal injection methods [8]. The moving boundary method also offers the advantage of simplicity as it does not require a zonal injection mechanism. However, for enzymes requiring multiple substrates, it is limited to those systems in which the enzyme possesses either a greater or a lesser net migration velocity than all of the required substrates.

Acknowledgments

Financial support was received from the National Institute of Health (Grant 25431) and PerSeptive Biosystems.

References

[1] J. Bao and F.E. Regnier, J. Chromatogr., 608 (1992) 217.
[2] D. Wu and F.E. Regnier, Anal. Chem., 65 (1993) 2029.
[3] K.J. Miller, I. Leesong, J. Bao, F.E. Regnier and F.E. Lytle, Anal. Chem., 65 (1993) 3267.
[4] D. Wu, F.E. Regnier and M.C. Linhares, J. Chromatogr. B, 657 (1994) 357.
[5] L.Z. Avila and G.M. Whitesides, J. Org. Chem., 58 (1993) 5508.
[6] Q. Xue and E.S. Yeung, Anal. Chem., 66 (1994) 1175.
[7] B.J. Harmon, D.H. Patterson and F.E. Regnier, Anal. Chem., 65 (1993) 2655.
[8] B.J. Harmon, I. Leesong and F.E. Regnier, Anal. Chem., 66 (1994) 3797.
[9] B.J. Harmon, D.H. Patterson and F.E. Regnier, J. Chromatogr. A, 657 (1993) 429.
[10] D.H. Patterson, B.J. Harmon and F.E. Regnier, J. Chromatogr. A, 662 (1994) 389.
[11] H.-T. Chang and E.S. Yeung, Anal. Chem., 65 (1993) 2947.
[12] S. Liu and P.K. Dasgupta, Anal. Chim. Acta, 268 (1992) 1.
[13] S. Liu and P.K. Dasgupta, Anal. Chim. Acta, 283 (1993) 739.
[14] P.K. Dasgupta and S. Liu, Anal. Chem., 66 (1994) 1792.
[15] C.A. Monnig and J.W. Jorgenson, Anal. Chem., 63 (1991) 802.
[16] J. Pawliszyn and J. Wu, J. Chromatogr., 559 (1991) 111.
[17] J. Wu and J. Pawliszyn, Talanta, 39 (1992) 1281.
[18] L.Z. Avila, Y.-H. Chu, E.C. Blossey and G.M. Whitesides, J. Med. Chem., 36 (1993) 126.
[19] Y.-H. Chu, L.Z. Avila, H.A. Biebuyck and G.M. Whitesides, J. Med. Chem., 35 (1992) 2915.
[20] C. Schwer and F. Lottspeich, J. Chromatogr., 623 (1992) 345.
[21] P. Gebauer, W. Thormann and P. Bocek, J. Chromatogr., 608 (1992) 47.
[22] R. Aebersold and H.D. Morrison, J. Chromatogr., 516 (1990) 79.